American Mineralogist, Volume 78, pages 1165–1173, 1993

Modulated microstructure in synthetic majorite

Yanbin Wang, Tibor Gasparik, Robert C. Liebermann
NSF Center for High Pressure Research and Department of Earth and Space Sciences,
State University of New York at Stony Brook, Stony Brook, New York 11794, U.S.A.

Abstract

Transmission electron microscopy on Mg end-member majorite crystals synthesized at 22 GPa and above 2350 °C reveals a modulated microstructure, characterized by mutually intersecting linear contrasts parallel to the tetragonal {101} planes, with a typical wavelength of the modulation between 150 and 300 Å. Streaking perpendicular to the {101} planes is observed in electron diffraction patterns. The modulated microstructure coarsens with decreasing synthesis and quench temperature and, by 2050 °C, is completely replaced by twin domains related by reflection operations across the tetragonal {101} planes.

These observations suggest that the structural modulation is due to a phase transformation in majorite from cubic (space group $Ia3d$) to tetragonal ($I4_1/a$) near 2350 °C, probably through ordering of the $^{[6]}$Mg and $^{[6]}$Si atoms. The observed microstructure is a result of partial inversion during quenching from above 2350 °C and reflects a transitional state in which the cubic structure is perturbed by a number of intersecting wave systems of strain modulation. Majorite specimens found in meteorites reportedly have cubic symmetry, whereas most of those synthesized in the laboratory are tetragonal; this discrepancy may be reconciled by the phase transformation.

Introduction

At pressures between 16 and 23 GPa and temperatures above 1600 °C, $MgSiO_3$ crystallizes as a garnet phase, known as majorite $[Mg_3^{[8]}(MgSi)^{[6]}Si_3^{[4]}O_{12}]$. We shall refer to it as Mg end-member majorite to distinguish it from the more general majorite, $Mg_3(Fe,Al,Si)_2Si_3O_{12}$. Majorite garnet is considered to be a major constituent of the transition zone of the Earth's mantle (Ringwood, 1967; Liu, 1977; Akaogi and Akimoto, 1977; Ito and Takahashi, 1987; Gasparik, 1990); its physical properties therefore have great geophysical importance for this region of the Earth (Jeanloz, 1981; Hatch and Ghose, 1989; McMillan et al., 1989; Hofmeister and Chopelas, 1991).

Results of single-crystal X-ray diffraction (Angel et al., 1989) indicate that Mg end-member majorite synthesized at 18 GPa and 1800 °C and recovered at ambient conditions exhibits tetragonal symmetry (space group $I4_1/a$), with Mg and Si atoms preferentially occupying the octahedrally coordinated Oc1(Mg3) and Oc2(Si1) sites, respectively (Table 1 and Fig. 1). Most of the powder X-ray studies on synthetic Mg-Fe-rich majorite crystals with Fe contents defined by $x\,[Fe_{tot}/(Mg + Fe)_{tot}]$ up to ~0.24 are consistent with this space group (Kato and Kumazawa, 1985; Kato, 1986; Sawamoto, 1987; Matsubara et al., 1990; Ohtani et al., 1991). However, some of the Fe-enriched majorite crystals ($x > 0.2$) synthesized by Kato (1986) reportedly have cubic symmetry. No cubic-structured Mg end-member majorite has been reported, although results from single-crystal X-ray diffraction (Angel et al., 1989) and polycrystalline ^{29}Si MAS NMR spectroscopy (Phillips et al., 1992) indicate a certain degree of disorder of Mg and Si on the two sites in the tetragonal crystals. On the other hand, natural Mg-Fe-rich majorite with $x \geq 0.2$ found in meteorites reportedly has cubic symmetry, with space group $Ia3d$ (Binns et al., 1967; Mason et al., 1968; Jeanloz, 1981; McMillan et al., 1989), in which the $^{[6]}$Mg and $^{[6]}$Si atoms are randomly distributed (Table 1).

On the basis of group theoretical arguments, Hatch and Ghose (1989) suggested that the tetragonal structure of Mg end-member majorite can be derived from the cubic structure through ordering of the $^{[6]}$Mg and $^{[6]}$Si atoms. They further proposed that the cubic phase may be stable at high temperatures and that the tetragonal majorite is a quench product. Their suggestion is largely based on the observed twinning in majorite reported by Angel et al. (1989), who pointed out, however, that such an ordering process is unlikely to be completed within the few seconds it takes to quench an experiment.

The question of whether a disordered cubic phase exists in Mg end-member majorite may have significant geophysical importance, because order-disorder transformations are commonly associated with changes in physical and thermodynamic properties (e.g., Salje, 1990). One particular signature of such phase transitions is the microstructure. The ordering processes in minerals and alloys are generally sluggish and therefore often result in a modulated texture in the quenched crystals characteristic of partial inversion (McConnell, 1965, 1971, 1975; Tanner et al., 1982). Such information is particularly valuable for majorite, which is stable only at high pressures and temperatures, making direct measurements difficult.

In this paper, we report transmission electron micros-

0003–004X/93/1112–1165$02.00

Table 1. Atomic positions for tetragonal ($I4_1/a$) and possible cubic ($Ia3d$) Mg end-member majorite, $Mg_3^{[8]}(MgSi)^{[6]}Si_3^{[4]}O_{12}$

	Cubic ($Ia3d$)*				Tetragonal ($I4_1/a$)*,**			
Site†	Atom	Position	Symmetry	Coordinates	Atom	Position	Symmetry	Coordinates
D	Mg	24(c)	222	⅛, 0, ¼	Mg1	16(f)	1	~⅛, ~0, ~¼‡
					Mg2	8(e)	2	0, ¼, ~⅝
Oc	Mg, Si	16(a)	$\bar{3}$	0, 0, 0	Mg3	8(d)	$\bar{1}$	0, 0, ½
					Si1	8(c)	$\bar{1}$	0, 0, 0
T	Si	24(d)	$\bar{4}$	⅛, 0, ¾	Si2	4(b)	$\bar{4}$	0, ¼, ⅜
					Si3	4(a)	$\bar{4}$	0, ¼, ⅞
					Si4	16(f)	1	~⅛, ~0, ~¾
Oxg	O	96(h)	1	x, y, z	O1	16(f)	1	x_1, y_1, z_1
					O2	16(f)	1	x_2, y_2, z_2
					O3	16(f)	1	x_3, y_3, z_3
					O4	16(f)	1	x_4, y_4, z_4
					O5	16(f)	1	x_5, y_5, z_5
					O6	16(f)	1	x_6, y_6, z_6

* From Prewitt and Sleight (1969).
** After Angel et al. (1989).
† D: dodecahedral; Oc: octahedral; T: tetrahedral; Oxg: oxygen.
‡ The ~ indicates approximate positions.

copy (TEM) observations on Mg end-member majorite synthesized at various temperatures up to 2500 °C. We have observed a modulated microstructure in crystals quenched from $T \geq 2350$–2400 °C, consistent with a cubic-tetragonal transformation; electron diffraction data also suggest coexistence of the cubic and tetragonal structures in these high-temperature specimens. On the basis of these observations, we conclude that a disordered, cubic phase may exist for Mg end-member majorite at $T \geq 2350$ °C and $P = 22$ GPa.

Experimental techniques

Well-sintered polycrystalline specimens containing crystals of Mg end-member majorite were synthesized at about 22 GPa and 2050–2500 °C in a 2000-ton Uniaxial split-sphere apparatus (USSA-2000) during a study of phase relations in the $MgSiO_3$ system (Gasparik, 1990). The synthesis conditions, starting materials, and major phases present in each experimental product are summarized in Table 2 (see Gasparik, 1990, for experimental details). Among the three experiments, no. 907 lasted for 6 h and contained an equal molar mixture of PbO and PbF_2, which were melted during the experiment. Electron microprobe analyses of the sample indicate no detectable Pb and F in the majorite crystals, suggesting that the flux did not affect thermodynamic stability of the sample. The other two samples were produced at much higher temperatures, and melting was observed near the hot spot, as indicated by a characteristic quench texture (Gasparik, 1990). Note that the melts have an average composition of $En_{60}Fo_{40}$ (in weight percent), in contact with the majorite. Gasparik (1990) estimated that melting temperature for Mg end-member majorite is about 2600 °C at 22.5 GPa.

Previous studies have demonstrated that in the cell assembly used for synthesis experiments, there is a strong axial temperature gradient, with a temperature difference of about 200 °C between the hot spot and cold end (e.g., Gasparik, 1989, 1990). This is advantageous in the present study, because variations in microstructure may be seen within a single specimen. In the two specimens that contained melts, maximum temperatures in the unmelted portions were estimated to be about 50–100 °C lower than the hot-spot temperatures listed in Table 2.

Standard 30-μm thin sections were made along the axial direction of the specimens, parallel to the thermal gradient. Optical microscopy on specimen no. 911 showed that there is a well-defined boundary between the melts (represented by a quench texture) and the solid phases (large majorite crystals). The unmelted portions of the specimens were then Ar-ion milled at 5 kV and 0.5 mA, and the thin foils were C coated. TEM observations were performed using a Jeol 200 CX electron microscope operating at 200 keV.

TEM observations

Figure 2A is a selected-area electron diffraction (SAED) pattern taken from specimen no. 907 (2050 °C); it is taken from the entire area shown in Figure 3A (with a slightly different orientation). Nearly periodic domains are present in Figure 3A, and the corresponding SAED patterns for domains a and b are shown in Figure 2B and 2C, respectively. Space group $I4_1/a$ requires the following diffraction conditions: [001] zone: $h, k = 2n$ for $hk0$, [100] zone: $k + l = 2n$ for $0kl$, where n is an integer. Thus Figure 2B is interpreted as along the [100] zone axis with spots of the $0k0$, $00l$, and $0kl$ types and Figure 2C along the [001] zone axis with diffraction spots of the $h00$, $0k0$, and $hk0$ types. These two orientations can be generated by a (101) reflection operation. Superposition of patterns a and b results in the intensity difference in the diffraction spots in Figure 2A. In sample no. 907 (quenched from 2050 °C), these {101} twins are lamellar twins with boundaries parallel to the {101} planes (Fig. 3A).

Also present are merohedral {110} twins; their existence can only be seen by selecting diffraction conditions

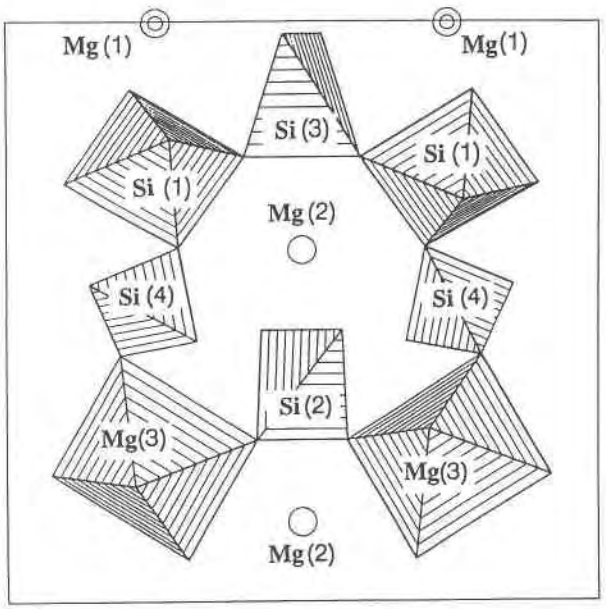

Fig. 1. A portion of the unit cell of tetragonal Mg end-member majorite projected along one of the **a** axes. Eightfold-coordinated Mg1 and Mg2 cations are represented by the circles; smaller octahedra are $Si1O_6$, with Si located at the center of the octahedra (site Oc2 in Table 1), and larger ones are $Mg3O_6$, with Mg at the centers (site Oc1 in Table 1).

TABLE 2. Synthesis conditions for Mg end-member majorite in this study

Expt.	Starting material*	*P* (GPa)	*T* (°C)**	*t* (h)	Major phases
907	B	21.9	2050	6.0	majorite ilmenite
911	D	22.4	2430	0.5	quench liquid majorite perovskite mod. spinel
926	G	22.6	2500	0.1	quench liquid majorite perovskite

* B = 1 mole MgO, 1.1 mole SiO_2, 0.05 mole PbO, 0.05 mole PbF_2; D = $En_{40}Fo_{60}$ (wt%); E = En_{100} (Fo = forsterite; En = enstatite).
** Hot-spot temperature. A temperature difference of up to 200 °C exists in the specimen.

$\mathbf{g}_{hkl}$ with $h \neq k$. The 240 reflection, in particular, has a substantially different structure factor than that for 420 (Angel et al., 1989). The {110} twins can be seen in Figure 3B, which is a dark field (DF) image taken under the diffraction condition $\mathbf{g} = 420$. They are observed in all of the specimens we have examined, regardless of the quench temperature.

Microstructure of the majorite specimens that are quenched from $T > 2400$ °C contrasts sharply with that of specimen no. 907. Figure 4A shows a typical microstructure for crystals quenched from 2500 °C (specimen no. 926). A modulated ("tweed") microstructure is present throughout the specimen, with contrast modulations approximately in the {101} planes, and the wavelength of the modulation about 150–300 Å. Elongation of the spots along the reciprocal ⟨101⟩* directions is observed in the SAED patterns taken from these crystals (indicated by double arrows in Fig. 4B). No coarse {101} twin domains are observed in specimen no. 926, although SAED patterns reveal intensity differences similar to those shown in Figure 2A, suggesting the presence of {101} twinning relations.

The modulated microstructure is also dominant in the specimen quenched from 2430 °C (specimen no. 911; Fig. 5A). In this case, we are able to observe microstructural variations from the hot spot toward the cold end over a distance of ~0.5 mm, corresponding to a temperature decrease of 100–150 °C. Figure 5A–5D are electron micrographs in the order of decreasing temperature. It can be seen that a coarse twin domain structure develops as quench temperature decreases, and the twins observed in Figure 5D (lowest temperature in specimen no. 911) are quite similar to those seen in specimen no. 907 (2050 °C), where no modulated contrast is observed. Superimposed on the coarse twin domains is the modulated structure in the specimen at 2430 °C, which becomes less visible in crystals near the low-temperature end of the specimen.

DISCUSSION

Domain formation in ordered alloys and minerals is commonly related to symmetry changes during order-disorder phase transitions (e.g., Van Tendeloo and Amelinckx, 1974; McConnell, 1971, 1988). Here we are interested in those transformations involving point-group symmetry changes. Group-theoretical analyses predict that such an order-disorder transformation produces microdomains in the ordered phase because of a symmetry loss, when the point group (H) of the ordered daughter phase is a subgroup of the disordered parent phase (G). Crystallographic orientations of the domains of the ordered phase are related by the symmetry elements that are absent in the ordered phase but present in the disordered one. These symmetry elements form a separate group (variant-generating group, V), which has no common elements with H other than the identity element. The number (n) of independent domain orientations (called orientation variants) is given by n = (order of G)/(order of H), and these orientation relations are uniquely defined for a given G and H pair (Amelinckx and Van Landyut, 1976). These results have been verified by numerous experimental data on systems with order-disorder relations.

The cubic space group $Ia3d$ (point group $m3m$) is the supergroup of space group $I4_1/a$ of the tetragonal phase (point group $4/m$) (Van Tendeloo and Amelinckx, 1974). The variant-generating group between the two phases can be either 32 or $3m$. However, point group $4/m$ is also a subgroup of another tetragonal point group, $4/mmm$, which itself is a subgroup of $m3m$. The variant-generat-

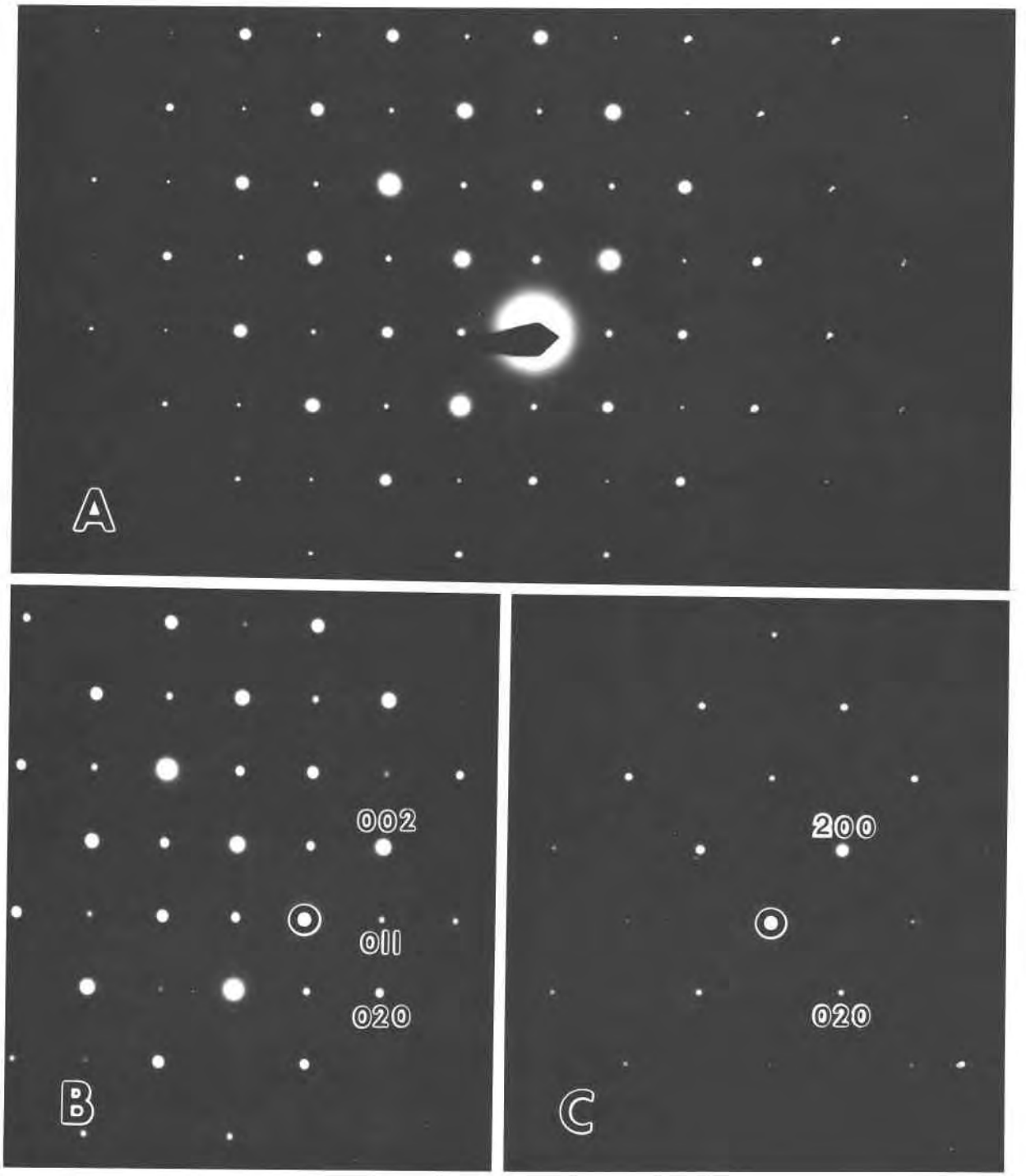

Fig. 2. (**A**) Selected area electron diffraction pattern of specimen no. 907; the corresponding image is shown in Fig. 3A. Note the intensity difference among diffraction spots. (**B**) and (**C**) SAED patterns of domains a and b, respectively, in Fig. 3A. Center spots circled. **B** is along the [001] and **C** along the [100] zone axes; the two domains thus have a (101) reflection twinning relation.

ing group between $4/mmm$ and $4/m$ can be either a twofold rotation perpendicular to, or a mirror plane containing, the fourfold axis. Thus, two types of twinning are expected from this symmetry consideration. The first is related to the symmetry change from $m3m$ to $4/mmm$ (V group: 3); this is threefold rotation twinning about the cubic body diagonal $\langle 111 \rangle$, which may be more conveniently described as pseudomerohedral twinning with

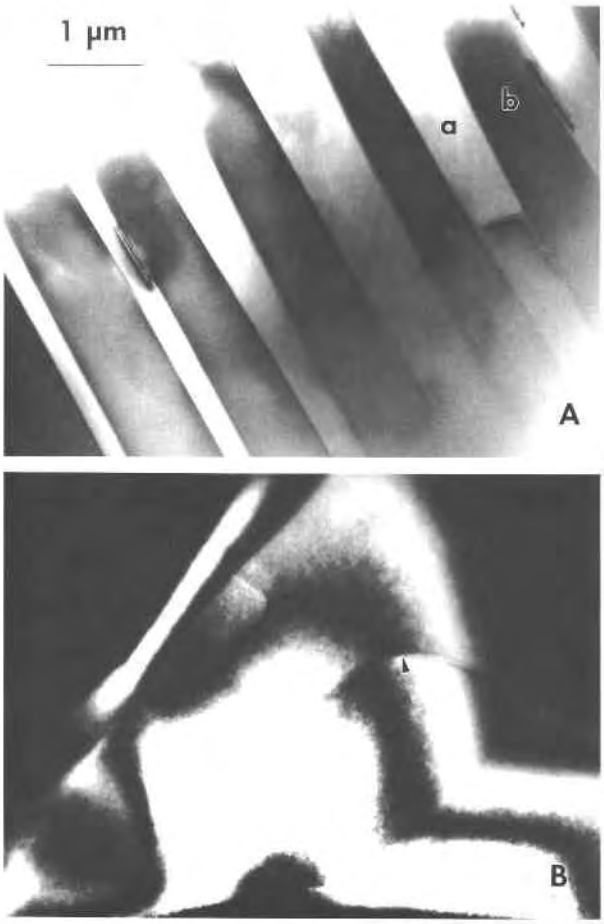

Fig. 3. Electron micrographs showing the morphologies of the {101} and {110} twins in Mg end-member majorite. (**A**) Bright field (BF) image of pseudomerohedral {101} twin domains observed in low-temperature specimen no. 907. All the domain boundaries are parallel to the {101} planes. (**B**) Dark-field (DF) image of merohedral (110) twin domains observed in specimen no. 926. The irregular, curved twin boundary is indicated by the arrow. Diffraction condition **g** = 420. Same scale for both **A** and **B**.

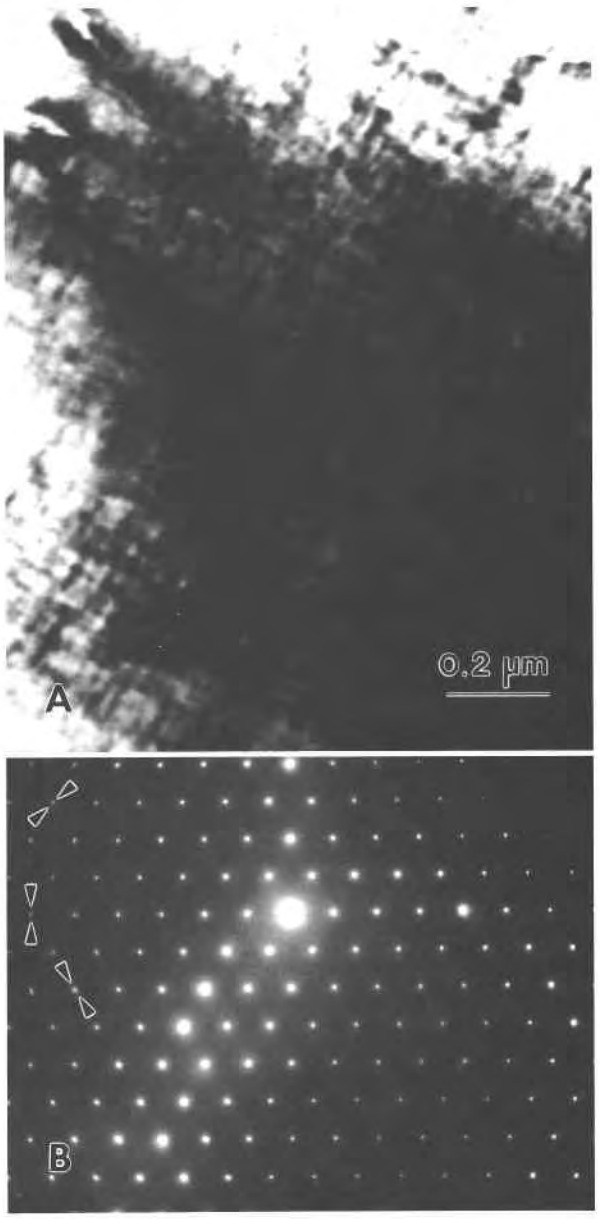

Fig. 4. Modulated microstructure observed in no. 926 (hot-spot temperature 2530 °C). (**A**) BF image showing a typical modulated microstructure, with modulations approximately parallel to the {101} planes. (**B**) SAED pattern taken from such a crystal. Note streaking in diffraction spots along the ⟨101⟩* direction (double arrows).

mirror operations across {101}, since the threefold rotation results in switching between the tetragonal *c* axis and one of the equivalent *a* axes. The other is related to the symmetry change from $4/mmm$ to $4/m$ (V-group 2 or *m*); this is merohedral twinning with reflection operations across the {110} planes, which are the mirror planes for the $m3m$ and $4/mmm$ point symmetries. Indeed, we have observed both twinning relations in the tetragonal Mg end-member majorite (also see Angel et al., 1989).

The structural modulations in majorite occur in directions parallel to the [4]{101} twin planes. This observation is best explained by the existence of a phase transformation in which degeneration of the symmetry from $Ia3d$ to $I4_1/a$ results in such a tweed pattern, which may be described by orthogonal transverse wave perturbations parallel to the {101} planes (McConnell, 1965, 1988). However, the presence of such modulated microstructure does not necessarily indicate that these crystals have undergone a phase transformation. For example, the tweed microstructure could be produced within the tetragonal stability field in the very first stage of crystal growth (because the difference in free energy between enstatite and tetragonal majorite is far greater than that between the tetragonal and cubic majorite) and may not represent the equilibrium state. One example is cordierite (Putnis,

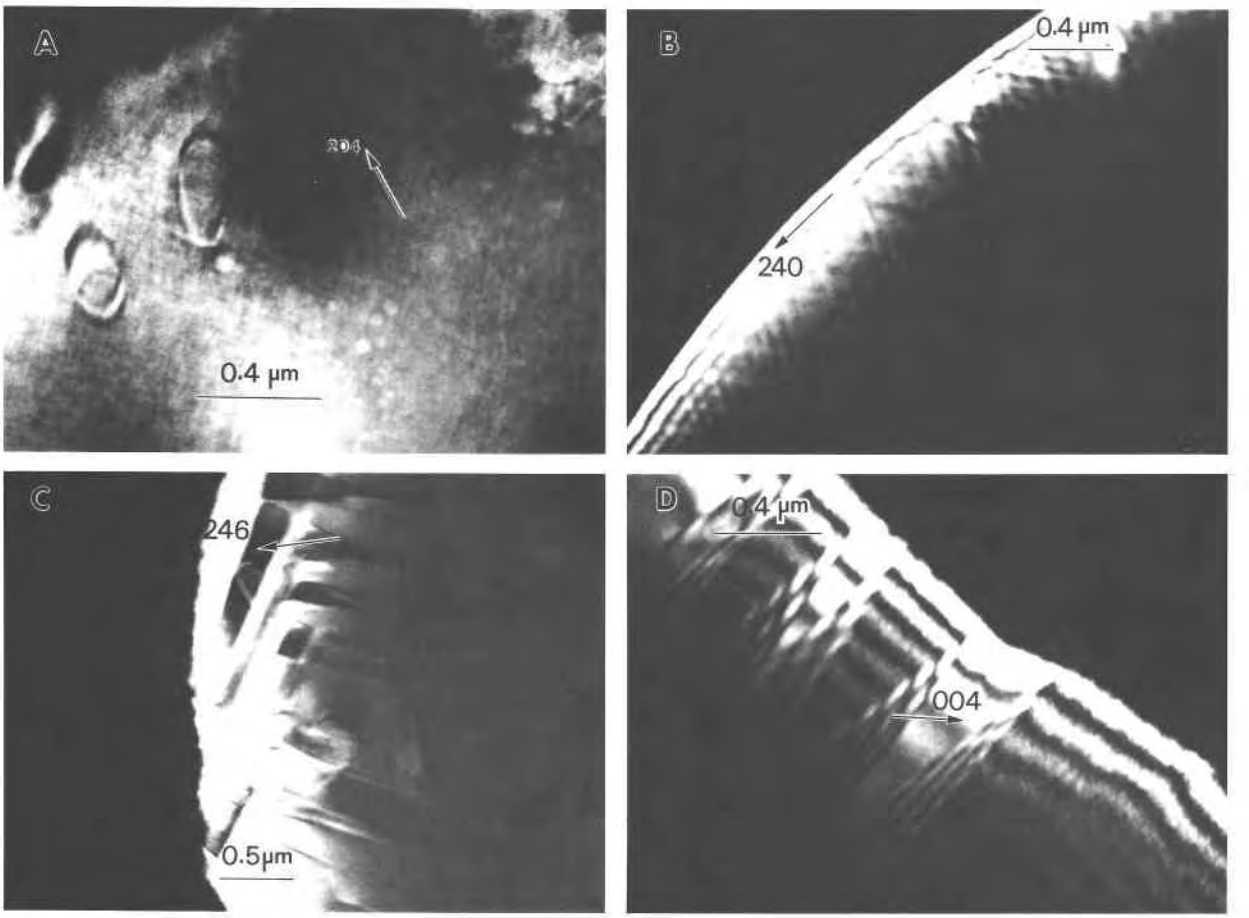

Fig. 5. A series of dark-field electron micrographs taken from specimen no. 911 (hot-spot temperature 2430 °C). **A–D** are presented in terms of decreasing quench temperature, illustrating the strain modulation as a function of quench temperature. Also notice the weak modulated contrast superimposed on coarse {101} twins in **C** and **D.** The diffraction conditions are marked on the figures.

1980). When synthesized from glass at temperatures below the hexagonal stability field, with increasing heating time, crystals evolve from hexagonal to modulated and finally to the stable orthorhombic structure with a high density of twins.

It is reasonable to assume that experiment no. 907 has reached equilibrium after 6 h at 2050 °C in the presence of flux (see Gasparik, 1990). The other two specimens, however, were synthesized with much shorter durations, but at much higher temperatures. Optical microscopy shows a clear boundary between majorite and quenched crystals in no. 911 (Gasparik, 1990). This observation and the fact that the coexisting quench liquid had a composition quite distinct from that of the adjacent majorite crystals suggest that the sample was quenched near the liquidus and was at least near equilibrium.

The microstructure variations in specimen no. 911 are quite similar to those observed in the cordierite described by Putnis (1980). However, in our case, the heating time is the same (30 min), but temperatures are different. Figure 5 is the key to understanding the cause of the microstructure: twins are observed in low-temperature regions, whereas tweeds exist in high-temperature portions of the sample. If the entire sample were in the tetragonal stability field, then twins would coarsen at a higher rate in higher temperature portions (similar to the long heating experiments in cordierite, when temperature is held constant); this is the opposite of what we observed. On the other hand, if the sample were entirely in the cubic stability field, then either tweed or the twinned microstructure would be dominant throughout the specimen after quench, depending on the rate of the ordering during quenching. Thus, we conclude that the microstructural variation observed in specimen no. 911 reflects near-equilibrium condition. Therefore, the tweed microstructure is due to the cubic-tetragonal ($Ia3d$-$I4_1/a$) phase transformation, as a result of partial inversion during quench from above ~2350 °C. Crystals transform to the $I4_1/a$ structure by ordering of the Mg and Si atoms in the octahedral sites when the temperature decreases (Table 1). An intermediate phase, $I4_1/acd$ (point group $4/mmm$), probably also exists but is not required in our interpretation of the observations. The boundary between the tweed and twins most probably corresponds to the phase boundary, whose temperature is estimated to be roughly 2300–2350 °C at 22 GPa.

TABLE 3. Reported crystal systems of majorite $(Mg,Fe)_3^{[8]}[(Mg,Fe)Si]^{[6]}Si_3^{[4]}O_{12}$

x^*	Reported crystal system	Source	Characterization techniques	References
~0.2	cubic	meteorite	XRD	1
		Tenham	TEM	2
~0.25	cubic	meteorite	XRD	3
		Coorara		
~0.22	cubic	meteorite	XRD, IR, NMR, Raman	4
		Catherwood	TEM	5
0.18–0.40	cubic	synthetic	XRD, Optical	6
		20 GPa,		
		1900–2100 °C		
0.0–0.18	noncubic	synthetic	Optical	7
		20 GPa		
		1900–2200 °C		
0.0	tetragonal	synthetic	XRD	8
		18–23 GPa		
		1800–2100 °C		
0.0–0.19	tetragonal	synthetic	XRD	9
		20 GPa, 2000 °C		
0.0–0.24	tetragonal	synthetic	XRD	10
		18 GPa, 1800 °C		

Note: references are as follows: 1 = Binns et al. (1967); 2 = Price et al. (1979); 3 = Mason et al. (1968); 4 = Jeanloz (1981); 5 = Madon and Poirier (1980); 6 = McMillan et al. (1989); 7 = Kato (1986); 8 = Sawamoto (1987); 9 = Matsubara et al. (1990); 10 = Ohtani et al. (1991).

* The $x = Fe_{tot}/(Mg + Fe)_{tot}$.

Although Hatch and Ghose (1989) reached the same conclusion, that a disordered cubic majorite may exist, their arguments were based on the presence of the pseudomerohedral twins observed by Angel et al. (1989). We demonstrate here that {101} twins are mainly primary in origin in all of our samples quenched from above 2050 °C. The majorite crystals studied by Angel et al. (1989) were synthesized at the much lower temperature of 1800 °C and are therefore most likely growth twins as well.

There is another piece of evidence that supports the existence of a disordered phase for Mg end-member majorite. Gasparik (1992) showed that along the enstatite–pyrope join, the garnet composition exhibits a strong temperature dependence, which can be best explained by increasing disorder of Mg, Si, and Al in the octahedral sites of the garnet structure. McMillan et al. (1989) studied cation disorder in garnets along this enstatite-pyrope join and confirmed that all of the intermediate garnets are disordered. All of these observations point to the possibility of disorder in Mg end-member majorite.

A certain degree of disorder has been independently observed in Mg end-member majorite synthesized at temperatures even below 2000 °C. Phillips et al. (1992) investigated cation ordering in majorite using ^{29}Si MAS NMR spectroscopy and found that crystals synthesized at 17.7 GPa and 2000 °C were mostly ordered, with ~12 (±3)% disorder on the Oc1 and Oc2 sites. Angel et al. (1989) performed single-crystal X-ray diffraction on a Mg end-member majorite sample synthesized at 1800 °C and found it to be 20 (±6)% disordered. In this latter case, a much smaller tetragonal distortion was observed, as indicated by the ratio of a/c (Angel et al., 1989), suggesting that the tetragonal distortion of the unit cell decreases with increasing degree of disorder. These results further suggest that the disorder in Mg end-member majorite may increase gradually within a rather wide temperature range until it eventually becomes completely disordered. Thus we observed a superposition of a coarse twin-domain structure and a modulated microstructure in Figure 5C and 5D.

SUMMARY AND IMPLICATIONS

We may now try to synthesize all of the available observations on Mg-Fe-rich majorite in terms of an $Ia3d$-$I4_1/a$ transformation (Table 3, Fig. 6). The crystal structure of these garnets depends on temperature as well as the Fe content, with temperatures of transition from tetragonal to cubic symmetry decreasing with increasing Fe content. Thus Kato (1986) observed cubic $Mg_{1-x}Fe_xSiO_3$ garnet with $x \geq 0.2$ at $T > 2000$ °C. We caution here, however, that Kato's observations were largely based on optical microscopy; a more thorough study is needed for the Fe-enriched majorite. High-temperature majorite crystals ($T > 2400$ °C) should also be studied more closely with spectroscopic techniques (e.g., NMR, IR, and Raman).

Disordered cubic majorite could be produced by shock events at temperatures exceeding the transition point or as a metastable product during the transformations from a low-pressure pyroxene-like structure to majorite. Tetragonal majorite might also exist in meteorites with appropriate thermal histories. Earlier structure determinations of majorite from meteorites may not have been accurate enough to resolve the tetragonal distortion; it would be very interesting to examine systematically the microstructure of these majorite crystals produced by shock events.

With the high transformation temperature (~2350 °C) for the cubic Mg end-member majorite, the stable garnet phase in the transition zone (~1500 °C and 13–22 GPa) should be tetragonal and should be at least partially or-

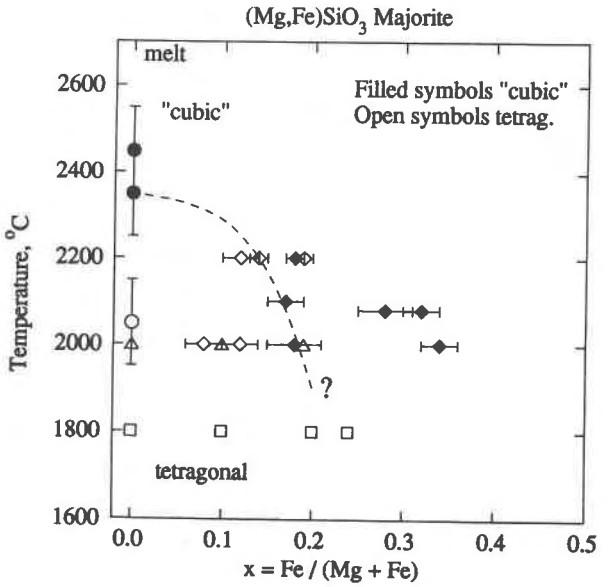

Fig. 6. *T-X* diagram compiled from available data on synthetic Mg-Fe silicate majorite. *X* defined as $Fe_{tot}/(Mg + Fe)_{tot}$ in the crystal. Solid symbols represent reportedly cubic majorite, open symbols tetragonal. Dashed curve with question mark is the speculative phase boundary between cubic and tetragonal majorite. Melting occurs above 2600 °C for $x = 0.0$. Circles from present study, diamonds from Kato (1986), triangles from Ohtani et al. (1991), and squares from Matsubara et al. (1990).

dered. However, since the transformation may occur gradually within a wide temperature range, physical properties of the tetragonal majorite may change significantly over the temperature range in the transition zone. The excess specific heat arising from the disorder is important to describe correctly the phase boundary between the majorite and ilmenite phases in the $MgSiO_3$ system (e.g., Figs. 2 and 3 of Gasparik, 1992). On the other hand, the transformation from $Ia3d$ to $I4_1/a$, being improper ferroelastic, could result in a decrease in selected elastic constants below the transition (Hatch and Ghose, 1989). A particularly interesting possibility is the behavior of c_{11}-c_{12}, which is affected by the Γ_3^+ mode during the order-disorder transition (see Hatch and Ghose, 1989). Tanner et al. (1982) have shown that for a large number of alloys, the tetragonal-cubic (order-disorder) transitions are characterized by an anomalous decrease in (tetragonal) c_{11}-c_{12} and a modulated texture when the transition temperature is approached from below, resulting in martensitic behavior. The c_{11}-c_{12} mode could be sensitive to temperature far below T_c; thus more studies are needed to understand the behavior of tetragonal majorite below the transformation.

Acknowledgments

The authors thank R. Angel, J. Fitz Gerald, and D. Palmer for helpful discussions. We thank J. Fitz Gerald for pointing out an error in the early indexing of one of the SAED patterns. We also thank D. Veblen, G. Guthrie, and an anonymous reviewer for constructive comments that greatly improved the manuscript. The high-pressure syntheses were conducted at the High Pressure Laboratory at Stony Brook, which is jointly supported by the State University of New York at Stony Brook and NSF grant EAR-89-17563; this laboratory is now part of the NSF Center for High Pressure Research (EAR-89-20239). The electron microscopy was carried out using a Jeol 200CX transmission electron microscope under the supervision of R.J. Reeder. This work was supported by NSF grants EAR-88-17097 and EAR-91-04563. MPI contribution no. 72.

References cited

Akaogi, M., and Akimoto, S. (1977) Pyroxene-garnet solid solution equilibria in the system $Mg_4Si_4O_{12}$-$Mg_3Al_2Si_3O_{12}$ and $Fe_4Si_4O_{12}$-$Fe_3Al_2Si_3O_{12}$ at high pressures and temperatures. Physics of the Earth and Planetary Interiors, 15, 90–106.

Amelinckx, S., and Van Landyut, J. (1976) Contrast effects at planar interfaces. In H.R. Wenk, Ed., Electron microscopy in mineralogy, p. 68–112. Springer-Verlag, Amsterdam.

Angel, R.J., Finger, L.W., Hazen, R.M. Kanzaki, M., Weidner, D.J., Liebermann, R.C., and Veblen, D.R. (1989) Structure and twinning of single-crystal $MgSiO_3$ garnet synthesized at 17 GPa and 1800 °C. American Mineralogist, 74, 509–512.

Binns, R.A., Davis, R.J., and Reed, S.J.B. (1967) Ringwoodite: Natural $(Mg,Fe)_2SiO_4$ spinel in the Tenham meteorite. Nature, 221, 943–944.

Gasparik, T. (1989) Transformation of enstatite-diopside-jadeite pyroxenes to garnet. Contributions to Mineralogy and Petrology, 102, 389–405.

——— (1990) Phase relations in the transition zone. Journal of Geophysical Research, 95, 15751–15769.

——— (1992) Melting experiments on the enstatite-pyrope join at 80–152 kbar. Journal of Geophysical Research, 97, 15181–15188.

Hatch, M.D., and Ghose, S. (1989) Symmetry analysis of the phase transition and twinning in $MgSiO_3$ garnet: Implications to mantle mineralogy. American Mineralogist, 74, 1221–1224.

Hofmeister, A.M., and Chopelas, A. (1991) Vibrational spectroscopy of end-member silicate garnets. Physics and Chemistry of Minerals, 17, 503–526.

Ito, E., and Takahashi, E. (1987) Ultrahigh pressure phase transformations and the constitution of the deep mantle. In M.H. Manghnani and Y. Syono, Eds., High pressure research in mineral physics, p. 221–229. American Geophysical Union, Washington, DC.

Jeanloz, R. (1981) Majorite: Vibrational and compressional properties of a high-pressure phase. Journal of Geophysical Research, 86, 6171–6179.

Kato, T. (1986) Stability relation of $(Mg,Fe)SiO_3$ garnets, major constituents in the Earth's interior. Earth and Planetary Science Letters, 77, 399–408.

Kato, T., and Kumazawa, M. (1985) Garnet phase of $MgSiO_3$ filling the pyroxene-ilmenite gap at very high temperature. Nature, 316, 803–805.

Liu, L. (1977) The system enstatite-pyrope at high pressures and temperatures and the mineralogy of the Earth's mantle. Earth and Planetary Science Letters, 36, 237–245.

Madon, M., and Poirier, J.-P. (1980) Dislocations in spinel and garnet high-pressure polymorphs of olivine and pyroxene: Implications for mantle rheology. Science, 207, 66–68.

Mason, B., Nelen, J., and White, J.S., Jr. (1968) Olivine-garnet transformation in a meteorite. Science, 160, 66–67.

Matsubara, R., Toraya, H., Tanaka, S., and Sawamoto, H. (1990) Precision lattice-parameter determination of $(Mg,Fe)SiO_3$ tetragonal garnets. Science, 247, 697–700.

McConnell, J.D.C. (1965) Electron optical study of effects associated with partial inversion in a silicate phase. Philosophical Magazine, 11, 1289–1301.

——— (1971) Electron-optical study of phase transformations. Mineralogical Magazine, 38, 1–20.

——— (1975) Microstructure of minerals as petrogenetic indicators. Annual Review of Earth and Planetary Sciences, 3, 129–155.

——— (1988) Symmetry aspects of pretransformation behavior in metallic alloys. Metallurgical Transactions, 19A, 159–167.

McMillan, P., Akaogi, M., Ohtani, E., Williams, Q., Nieman, R., and Sato, R. (1989) Cation disorder in garnets along the $Mg_3Al_2Si_3O_{12}$-

$Mg_4Si_4O_{12}$ join: An infrared, Raman and NMR study. Physics and Chemistry of Minerals, 16, 428–435.

Ohtani, E., Kagawa, N., and Fukino, K. (1991) Stability of majorite $(Mg,Fe)SiO_3$ at high pressures and 1800 °C. Earth and Planetary Science Letters, 102, 158–166.

Phillips, B.L., Howell, D.A., Kirkpatrick, R.J., and Gasparik, T. (1992) Investigation of cation order in $MgSiO_3$-rich garnet using ^{29}Si and ^{27}Al MAS NMR spectroscopy. American Mineralogist, 77, 704–712.

Prewitt, C.T., and Sleight, A.W. (1969) Garnet-like structures of high-pressure cadmium germanate and calcium germanate. Science, 163, 386–387.

Price, G.D., Putnis, A., and Agrell, S.O. (1979) Electron petrography of shock-produced veins in the Tenham chondrite. Contributions to Mineralogy and Petrology, 71, 211–218.

Putnis, A. (1980) The distortion index in anhydrous Mg-cordierite. Contributions to Mineralogy and Petrology, 74, 135–141.

Ringwood, A.E. (1967) The pyroxene-garnet transformation in the Earth's mantle. Earth and Planetary Science Letters, 2, 255–263.

Salje, E.K.H. (1990) Phase transitions in ferroelastic and co-elastic crystals, 366 p. Cambridge University Press, Cambridge, U.K.

Sawamoto, H. (1987) Phase diagram of $MgSiO_3$ at pressures up to 24 GPa and temperatures up to 2200 °C: Phase stability and properties of tetragonal garnet. In M.H. Manghnani and Y. Syono, Eds., High pressure research in mineral physics, p. 209–219. American Geophysical Union, Washington, DC.

Tanner, L.E., Pelton, A.R., and Gronsky, R. (1982) The characterization of pretransformation morphologies: Periodic strain modulations. Journal de Physique, C4, 169–172.

Van Tendeloo, G., and Amelinckx, S. (1974) Group-theoretical considerations concerning domain formation in ordered alloys. Acta Crystallographica, A30, 431–440.

Manuscript received September 22, 1992
Manuscript accepted July 13, 1993